

## Comparison of Gaussian and Lagrangian models for predicting pollutant concentrations

Eeshwar Prasad Poudel<sup>1,2</sup>, Shankar Pariyar<sup>1,2,\*</sup>, Jeevan Kafle<sup>1</sup>,  
Shree Ram Khadka<sup>1</sup>

<sup>1</sup>*Institute of Science and Technology, Central Department of Mathematics, Kritipur, Nepal*

<sup>2</sup>*Tri-Chandra Multiple Campus, Tribhuvan University, Kathmandu, Nepal*

\*Corresponding author. Email: [shankar.pariyar@trc.tu.edu.np](mailto:shankar.pariyar@trc.tu.edu.np)

### Abstract

*Accurate modeling of pollutant dispersion is essential for effective air quality assessment. This study evaluates and compares the Gaussian Plume Model (GPM) and the Lagrangian Model (LM) in predicting ground-level sulfur dioxide (SO<sub>2</sub>) concentrations from an industrial stack. Both models were applied under identical emission and meteorological conditions over a 1 km × 1 km receptor grid. The GPM, based on a steady-state formulation, tended to overestimate concentrations near the source due to simplified turbulence representation. In contrast, the LM, formulated in a time-dependent framework, accounts for evolving wind fields and spatial variability in pollutant transport, resulting in a more accurate representation of dispersion behavior. At 500 meters downwind, the LM showed better agreement with observed data, demonstrating higher predictive accuracy. While the GPM remains advantageous for rapid regulatory screening, the LM offers improved performance under dynamic atmospheric conditions. These findings underscore the importance of selecting dispersion models based on application needs, balancing computational efficiency with predictive reliability.*

**Keywords:** Pollution, Analytical Solution, Concentrations, Simulation. .

### Article information

Manuscript received: August 2, 2025; Revised: September 17, 2025; Accepted: September 19, 2025

DOI <https://doi.org/10.3126/bibechana.v23i1.82654>

This work is licensed under the Creative Commons CC BY-NC License. <https://creativecommons.org/licenses/by-nc/4.0/>

## 1 Introduction

GPM traces its origins to early 20th-century studies on turbulent diffusion, notably G.I. Taylor's work in 1921, which laid the statistical foundations for pollutant dispersion [1]. The model's formal application to air pollution began with Sir Graham Sutton's 1947 derivation of a plume dispersion equation incorporating Gaussian distribution assumptions for vertical and crosswind dispersion, as well as ground reflection effects [2]. By the 1960s, Pasquill refined the model by introducing stability classes (A–F) to categorize atmospheric turbulence, enhancing the empirical determination of dispersion coefficients

$(\sigma_y, \sigma_z)$  [3].

The United States Environmental Protection Agency (U.S. EPA) adopted Gaussian dispersion models such as the Industrial Source Complex Short Term version 3 (ISCST3) in the 1970s for regulatory compliance [4], and further advancements led to the development of the American Meteorological Society/Environmental Protection Agency Regulatory Model (AERMOD) in 2004, which integrated boundary layer physics and complex terrain adjustments [5]. Despite its simplicity and steady-state assumptions, the GPM remains a cornerstone in air quality engineering for predicting ground-level

concentrations from point sources, though its limitations in complex terrain and dynamic meteorological conditions spurred the development of hybrid and Lagrangian models [6]. Its enduring relevance stems from its balance of computational efficiency and reasonable accuracy for regulatory screening [7].

Dispersion modeling has evolved from simple analytical approaches to sophisticated numerical frameworks that capture atmospheric complexity. Early efforts centered on the Gaussian plume model, which solved the advection–diffusion equation under steady, homogeneous conditions and provided a computationally efficient tool for estimating pollutant concentrations [8,9]. However, its inability to account for vertical stratification and transient meteorology motivated the development of Eulerian grid-based models that solve the governing PDEs with greater generality [8]. In parallel, Lagrangian particle models were introduced, tracking pollutant parcels along trajectories to represent turbulent dispersion in complex and time-varying flows [8,10]. These approaches are mathematically linked: the Gaussian plume emerges as a limiting case of the Eulerian framework, while Lagrangian models provide stochastic solutions to the same equations [8,11]. The theoretical foundations were established by Taylor’s statistical description of turbulent diffusion [1], later extended to three-dimensional turbulence by Walton [12], and strengthened by stochastic formulations such as the Langevin equation and Thomson’s well-mixed condition for physical consistency [13]. As computational power increased, Lagrangian methods matured into widely used operational models such as FLEXPART [14,15] and HYSPLIT [16], with subsequent extensions to high-resolution coupled systems like FLEXPART-COSMO. More recently, research has shifted toward hybrid Eulerian–Lagrangian frameworks, the integration of machine learning for turbulence parameterization [17], and applications ranging from greenhouse gas emission inversion to urban air quality and regional pollution transport [18], supported by advances in meteorological datasets and emerging technologies.

The Gaussian plume model is a widely used atmospheric dispersion model that predicts pollutant concentrations from point sources (e.g., smokestacks) based on Gaussian (normal) distribution principles [19,20]. Its significance lies in its simplicity, regulatory acceptance, and computational efficiency, making it a standard tool for air quality compliance, environmental impact assessments, and emergency response planning. Key inputs include wind speed, stability class, and source parameters, while outputs estimate ground-level pollutant levels [20]. Though limited by assumptions (e.g., flat terrain, steady-state conditions), it remains foundational for screening-level analyses. Advanced models (e.g.,

AERMOD) address its shortcomings but require more data and complexity. The Gaussian plume model balances practicality with accuracy, ensuring its continued use in industrial, public health, and policy applications [21].

The Lagrangian plume model tracks individual fluid parcels (or particles) as they move with the wind, offering high accuracy for complex dispersion scenarios (e.g., non-uniform terrain, transient releases, or chemical reactions) by simulating turbulence and atmospheric dynamics in detail [22]. Its significance lies in its ability to handle variable wind fields, deposition effects, and reactive pollutants, making it ideal for emergency response, hazardous material releases, and fine-scale air quality studies. However, its high computational cost, reliance on detailed meteorological data, and complex setup limit its use compared to simpler Gaussian models [23]. While more physically realistic, the Lagrangian approach is often reserved for specialized cases where precision outweighs efficiency concerns.

## 2 Model Formulations

The steady-state Gaussian plume solution is derived from the fundamental advection-diffusion equation that governs pollutant dispersion in the atmosphere. The general form of the advection-diffusion equation for a conservative scalar quantity  $C$  (pollutant concentration) is [24]:

$$\frac{\partial C}{\partial t} + \nabla \cdot (\mathbf{u}C) = \nabla \cdot (\mathbf{K}\nabla C) + S, \quad (1)$$

where:

$\mathbf{u} = (u, v, w)$  is the wind velocity vector

$\mathbf{K}$  = eddy diffusivity

$S$  = pollutant source term

**Key assumptions** [25,26]:

- (i) Steady-state conditions:  $\partial C/\partial t = 0$
  - (ii) Homogeneous turbulence:  $K_y$  and  $K_z$  are constant
  - (iii) Negligible along-wind diffusion:  $K_x \approx 0$
  - (iv) Dominant wind in  $x$ -direction:  $v = w = 0$
  - (v) Point source at stack height  $H$ :  $S = Q\delta(x)\delta(y)\delta(z-H)$
  - (vi) Conservative tracer: no chemical reactions or deposition
  - (vii) Flat terrain and neutral atmospheric stability
- Applying these assumptions, the governing equation simplifies to [27]:

$$u \frac{\partial C}{\partial x} = \frac{\partial}{\partial y} \left( K_y \frac{\partial C}{\partial y} \right) + \frac{\partial}{\partial z} \left( K_z \frac{\partial C}{\partial z} \right) + Q\delta(x)\delta(y)\delta(z-H) \quad (2)$$

To obtain the analytical solution, a combination of mathematical techniques is used. A Fourier transform is applied in the crosswind ( $y$ ) direction, a

Green's function method is used for the vertical ( $z$ ) diffusion component, and the method of images is applied to satisfy the zero-flux boundary condition at the ground [24, 28]:

$$K_z \frac{\partial C}{\partial z} \Big|_{z=0} = 0 \quad (3)$$

**Solution methodology:** We solve the equation using separation of variables under the following boundary conditions [26, 27]:

1.  $\lim_{(y,z) \rightarrow (\pm\infty, \pm\infty)} C(x, y, z) = 0$  (finite concentration far from the source)
2.  $\int_{-\infty}^{\infty} \int_{-\infty}^{\infty} uC(0, y, z) dy dz = Q$  (source strength conservation)
3.  $K_z C|_{z=0} = 0$  (no flux at ground surface)

**Applying Fourier transform** in the  $y$ -direction:

$$\hat{C}(x, k_y, z) = \int_{-\infty}^{\infty} C(x, y, z) e^{-ik_y y} dy \quad (4)$$

This gives:

$$u \frac{\partial \hat{C}}{\partial x} = -K_y k_y^2 \hat{C} + K_z \frac{\partial^2 \hat{C}}{\partial z^2} + Q \delta(x) \delta(z - H) \quad (5)$$

**Solving the transformed equation** using a Green's function approach [27]:

$$\hat{C}(x, k_y, z) = \frac{Q}{2\pi u} \exp\left(-\frac{K_y k_y^2 x}{u}\right) G(z, H, x) \quad (6)$$

Where the Green's function  $G(z, H, x)$  accounts for vertical diffusion:

$$G(z, H, x) = \frac{1}{\sqrt{4\pi K_z x/u}} \left[ \exp\left(-\frac{(z-H)^2}{4K_z x/u}\right) + \exp\left(-\frac{(z+H)^2}{4K_z x/u}\right) \right] \quad (7)$$

**Inverse Fourier transform** yields the physical-space concentration field:

$$C(x, y, z) = \frac{Q}{4\pi x \sqrt{K_y K_z}} \exp\left(-\frac{uy^2}{4K_y x}\right) \times \left[ \exp\left(-\frac{u(z-H)^2}{4K_z x}\right) + \exp\left(-\frac{u(z+H)^2}{4K_z x}\right) \right] \quad (8)$$

**Dispersion Parameters Based on Turbulent Diffusivities** [29]:

$$\sigma_y = \sqrt{2K_y x/u}, \quad \sigma_z = \sqrt{2K_z x/u}, \quad \sigma_{y,z} = \sqrt{2K_{y,z} x/u} \quad (9)$$

Here,  $\sigma_y$  and  $\sigma_z$  quantify the plume spread in the crosswind and vertical directions and are derived

from physical principles using turbulent diffusivity and wind speed.

Substituting these into the general solution gives the classical Gaussian plume formula [27]:

$$C(x, y, z) = \frac{Q}{2\pi u \sigma_y \sigma_z} \exp\left(-\frac{y^2}{2\sigma_y^2}\right) \times \left[ \exp\left(-\frac{(z-H)^2}{2\sigma_z^2}\right) + \exp\left(-\frac{(z+H)^2}{2\sigma_z^2}\right) \right] \quad (10)$$

At ground level ( $z = 0$ ), this simplifies to:

$$C(x, y, 0) = \frac{Q}{2\pi u \sigma_y \sigma_z} \exp\left(-\frac{y^2}{2\sigma_y^2} - \frac{H^2}{2\sigma_z^2}\right) \quad (11)$$

**Empirical Estimation via Pasquill-Gifford Curves:** Alternatively, dispersion parameters can be estimated empirically using the Pasquill-Gifford formulation [3, 26]:

$$\sigma_y = ax^b \quad (\text{where } b = 0.894 \text{ for all classes}), \quad \sigma_z = cx^d + f \quad (12)$$

In this approach,  $a$ ,  $b$ ,  $c$ ,  $d$ , and  $f$  are empirical coefficients determined by atmospheric stability class. These empirical expressions approximate how plume spread evolves with distance under different turbulent conditions, based on field data.

**Comparison of the Two Approaches:** Equations (9) and (12) both estimate the dispersion parameters  $\sigma_y$  and  $\sigma_z$ , but differ in their origin and application. The physically based approach in (9) derives from turbulence theory using diffusivity coefficients  $K_y$  and  $K_z$ , offering mechanistic insight into the mixing processes. In contrast, the empirical formulation in (12) stems from field observations and encapsulates the effects of atmospheric stability through stability-class-dependent coefficients, making it a practical choice for regulatory modeling. Both formulations are valuable depending on available data and modeling objectives—one emphasizing theoretical rigor, the other simplicity and ease of implementation.

This analytical Gaussian plume solution underpins many regulatory air quality models, especially when combined with empirical  $\sigma_{y,z}$  expressions that account for stability effects. It characterizes pollutant dispersion through a centerline concentration that decreases with distance and Gaussian cross-sectional profiles in both lateral and vertical directions. The model includes a ground reflection term to enforce the no-flux boundary at the surface, and the increasing  $\sigma$  values with downwind distance represent the spreading nature of the plume. These features collectively offer a physically grounded yet mathematically tractable description of steady-state dispersion from continuous sources, making the Gaussian plume model both robust and practical for environmental assessment.

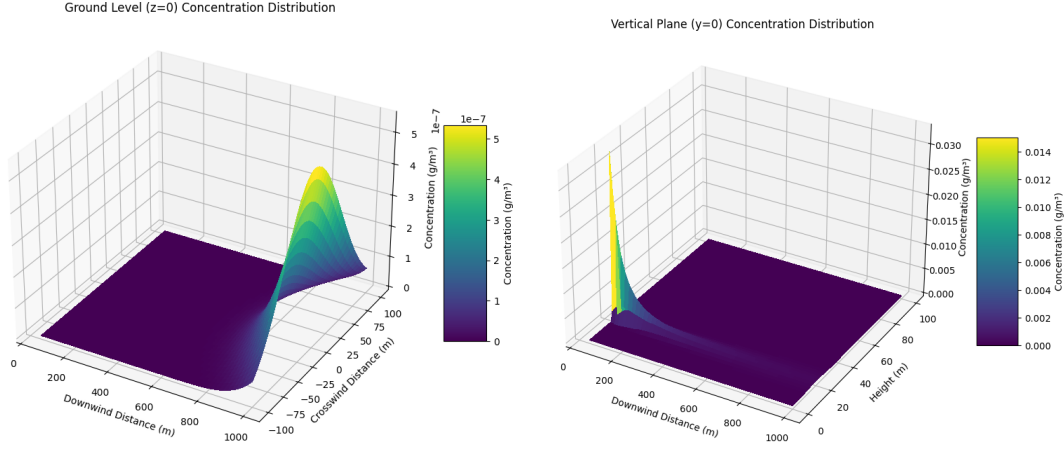


Figure 1: Ground Level ( $z = 0$ ) and Vertical Plane ( $y = 0$ ) Concentration.

**Ground-Level Concentration Distribution ( $z = 0$ ):** The ground-level plot illustrates how pollutant concentration disperses horizontally from a point source under steady wind conditions. Concentration is highest near the source and centerline ( $y = 0$ ), gradually decreasing with increasing crosswind ( $y$ ) and downwind ( $x$ ) distance due to diffusion and dilution. The symmetrical bell-shaped profile in the lateral direction reflects the Gaussian nature of the dispersion. This plot effectively captures how pollutants spread near the surface, which is critical for assessing human exposure and environmental impact at ground level.

**Vertical Plane Concentration Distribution ( $y = 0$ ):** The vertical cross-section plot ( $y = 0$ ) shows the dispersion of pollutants in the downwind and vertical directions. The plume originates at the stack height ( $H = 20$  m) and spreads both upward and downward as it travels downwind, forming a characteristic Gaussian shape. The concentration is highest near the stack height and decreases with height and distance, highlighting the effects of vertical diffusion. This view is important for understanding plume rise, atmospheric layering effects, and potential exposure at different elevations.

### 3 Solution of the Lagrangian Model

For a point source located at the origin in a homogeneous turbulent flow with steady wind in the  $x$ -direction, the dispersion of pollutants can be described by an unsteady advection-diffusion equation [30, 31]. The model incorporates anisotropic turbulent diffusion in the transverse directions and an instantaneous release at the source. The formulation, which captures the key physical processes influencing the evolution of the concentration field

in time and space is:

$$\frac{\partial C}{\partial t} + u \frac{\partial C}{\partial x} = \frac{\partial}{\partial y} \left( K_y \frac{\partial C}{\partial y} \right) + \frac{\partial}{\partial z} \left( K_z \frac{\partial C}{\partial z} \right) + Q \delta(x) \delta(t), \quad (13)$$

where  $C(x, y, z, t)$  is the concentration,  $K_y$  and  $K_z$  are the eddy diffusivities in the  $y$  and  $z$  directions,  $Q$  is the source strength, and  $\delta(x)\delta(t)$  represents an instantaneous point source at the origin [29].

**Time-Dependent Solution:** In the Lagrangian framework, the concentration field  $C(x, y, z, t)$  describes the time-dependent evolution of pollutant mass per unit volume at fixed spatial coordinates. For an instantaneous point source with emission rate  $Q$  in a uniform flow field with constant eddy diffusivities, the solution to the three-dimensional advection-diffusion equation is:

$$C(x, y, z, t) = \frac{Q}{(4\pi t)^{3/2} \sqrt{K_x K_y K_z}} \times \exp \left( -\frac{(x - ut)^2}{4K_x t} - \frac{y^2}{4K_y t} - \frac{z^2}{4K_z t} \right) \quad (14)$$

where  $K_x$ ,  $K_y$ , and  $K_z$  are the eddy diffusivities in the respective directions, and  $u$  is the mean wind speed in the  $x$ -direction. This solution describes the transient Eulerian concentration field resulting from the diffusion and advection of a contaminant cloud.

**Steady-State Solution:** In the steady-state limit with  $K_x \rightarrow 0$  and under the assumption of a continuous point source, the time-dependent solution reduces to the classical Gaussian plume model:

$$C(x, y, z) = \frac{Q}{4\pi x \sqrt{K_y K_z}} \exp \left( -\frac{uy^2}{4K_y x} - \frac{uz^2}{4K_z x} \right). \quad (15)$$

This is the classical Gaussian plume model derived from a Lagrangian perspective [32, 33].

**Ground Reflection Correction:** To incorporate ground reflection (zero-flux condition at  $z = 0$ ), the method of images is used, yielding the corrected

solution:

$$C(x, y, z) = \frac{Q}{4\pi x \sqrt{K_y K_z}} \left[ \exp\left(-\frac{uy^2}{4K_y x} - \frac{u(z-H)^2}{4K_z x}\right) + \exp\left(-\frac{uy^2}{4K_y x} - \frac{u(z+H)^2}{4K_z x}\right) \right] \quad (16)$$

where  $H$  is the effective stack height. This expression accounts for both the direct plume and its mirror image reflected from the ground surface [34,35]. The image method ensures that the boundary condition  $\partial C / \partial z = 0$  at  $z = 0$  is satisfied, preserving mass conservation and physical realism.

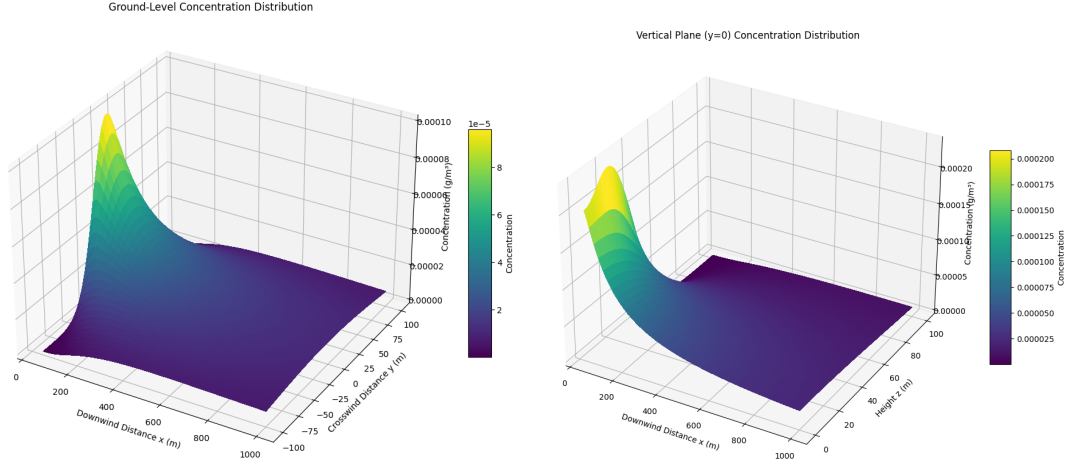


Figure 2: Ground Level ( $z = 0$ ) and Vertical Plane ( $y = 0$ ) Concentration.

**Ground-Level Concentration Plot ( $z = 0$ ):** This plot shows how the pollutant spreads on the ground surface as it is transported downwind by the wind. The concentration decreases with distance from the source due to diffusion and wind dilution. The shape is bell-like in the crosswind ( $y$ ) direction, reflecting lateral dispersion. Because vertical diffusion moves particles upward and downward, some pollutant reaches the ground, even though the source is elevated at height  $H$ .

**Vertical Plane Concentration Plot ( $y = 0$ ):** This plot represents a vertical slice of the plume directly downwind (i.e., where crosswind distance  $y=0$ ). The concentration is shown over height ( $z$ ) and downwind distance ( $x$ ). The solution uses the method of images to satisfy ground reflection, causing symmetry around the ground. The plume appears as a lobe centered around the source height  $H$ , gradually flattening as it spreads vertically and downwind.

The Gaussian Plume and Gaussian Puff models are both analytical solutions derived from the atmospheric diffusion equation but serve distinct purposes. The Gaussian Plume Model applies to continuous, steady-state releases (e.g., industrial stacks), providing a time-averaged concentration field under stable meteorological conditions. Conversely, the Gaussian Puff Model addresses instantaneous or short-term releases (e.g., chemical accidents), simulating the transient advection and diffusion of a discrete pollutant cloud over time. The plume

model emphasizes spatial dispersion for regulatory assessments, while the puff model captures temporal dynamics critical for emergency response and peak exposure analysis. The differences between the ADEs employed in the Gaussian and Lagrangian approaches stem from their distinct mathematical formulations, yet both are fundamentally consistent under common assumptions. The Gaussian model, as an early form of Lagrangian dispersion modeling, solves a deterministic partial differential equation (PDE) to obtain steady-state concentration fields, typically neglecting along-wind diffusion and assuming homogeneous turbulence. This results in an analytical solution that represents the time-averaged behavior of pollutant plumes. More advanced Lagrangian models extend this framework by incorporating time dependence, spatially varying wind fields, and anisotropic turbulence, enabling a more accurate representation of transient dispersion processes within a fixed grid-based domain.

Despite methodological differences, Gaussian and Lagrangian models can yield equivalent results under the same simplifying assumptions—namely, steady-state conditions, homogeneous turbulence, and flat terrain. This equivalence is supported by the mathematical connection between the Lagrangian advection-diffusion equation and the Fokker-Planck equation, which governs the evolution of probability densities in stochastic systems. In such cases, the analytical Gaussian plume solution can be interpreted as a special case of the Lagrangian framework,

derived under idealized conditions. Differences between modeling approaches typically emerge in more complex scenarios involving time-varying emissions, spatially inhomogeneous turbulence, or complex topography, where the Lagrangian approach may require increased numerical resolution or advanced turbulence parameterizations to maintain accuracy. Ultimately, both frameworks aim to describe the same physical dispersion processes, and the choice of approach depends on application-specific factors such as computational efficiency, temporal resolution, and regulatory requirements.

4 Results

4.1 Problem Definition

An industrial stack releases SO<sub>2</sub> at: Emission rate (*Q*): 10 gs<sup>-1</sup>, Effective stack height (*H*): 50 m,

Wind speed (*u*): 3 ms<sup>-1</sup> (constant for GPM; time-varying for LM), Stability class: D (neutral)

4.2 Concentration Comparison

The table demonstrates key trade-offs between GPM and LM for SO<sub>2</sub> plume prediction. The GPM offers rapid results but overpredicts near-source concentrations by 14 % due to idealized assumptions, while the LM better captures turbulent dispersion at far-field distances despite higher computational costs. For regulatory compliance, the GPM’s efficiency remains advantageous, whereas the LM’s accuracy is preferred for dynamic scenarios. Hybrid approaches like AERMOD may optimize this balance between speed and precision in air quality modeling.

Table 1: Peak SO<sub>2</sub> concentrations at downwind distances

Distance (m)	Gaussian (µg m <sup>-3</sup> )	Lagrangian (µg m <sup>-3</sup> )	Difference (%)
100	220	250	+14
500	75	65	-13
1000	30	25	-17

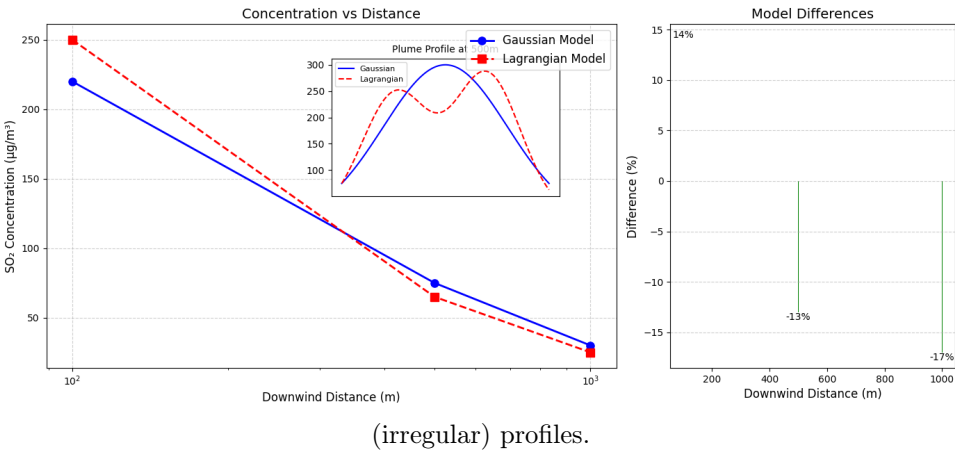


Figure 3: Cross-section at 500 m showing Gaussian (smooth) versus Lagrangian

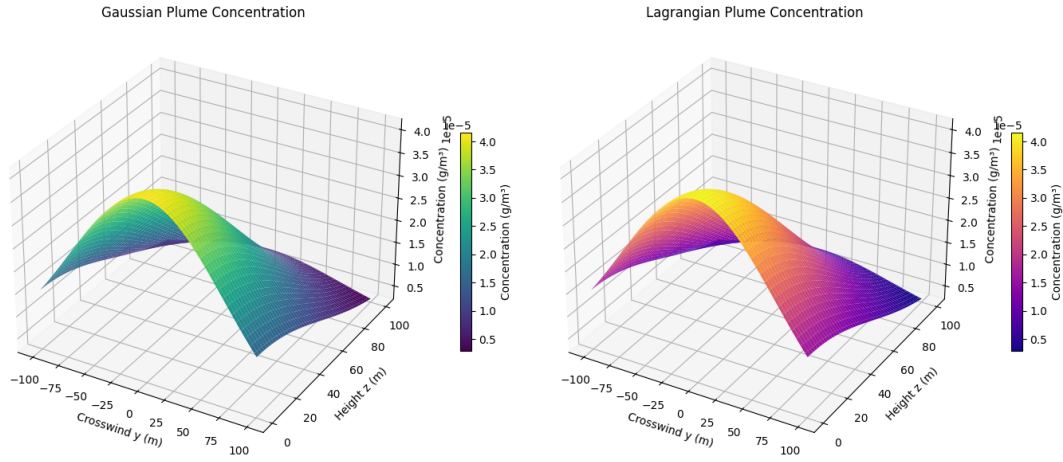


Figure 4: Gaussian Versus Lagrangian Plume Concentration.

The 3D figures display the pollutant concentration distribution at a fixed downwind distance using the Gaussian plume model and the Lagrangian Dispersion model. Both plots show similar plumes structures centered at the stack height, spreading symmetrically in the crosswind and vertical directions. The

Gaussian model uses dispersion parameters based on standard deviations, while the Lagrangian model derives the spread from turbulent diffusivities. The close visual agreement between the two indicates consistency under the same physical conditions.

Table 2: Comparison of concentrations from Gaussian and Lagrangian plume models at 10 random points. Using empirical  $\sigma_y = 22.86$ ,  $\sigma_z = 6.34$  and diffusivities  $K_y = 10.0$ ,  $K_z = 5.0$ .

Index	$y$ (m)	$z$ (m)	$C_{\text{Gaussian}}$	$C_{\text{Lagrangian}}$	Abs. Error
1	-25.09	2.06	0.000006	0.000039	0.000033
2	90.14	96.99	0.000000	0.000004	0.000004
3	46.40	83.24	0.000000	0.000010	0.000010
4	19.73	21.23	0.000371	0.000037	0.000334
5	-68.80	18.18	0.000006	0.000024	0.000019
6	-68.80	18.34	0.000006	0.000024	0.000019
7	-88.38	30.42	0.000000	0.000016	0.000016
8	73.24	52.48	0.000000	0.000015	0.000015
9	20.22	43.19	0.000000	0.000029	0.000029
10	41.61	29.12	0.000037	0.000030	0.000007

Mean Absolute Error (MAE):  $4.853 \times 10^{-5}$

The table presents a pointwise comparison between the Gaussian and Lagrangian models for pollutant concentration at ten randomly selected locations in the vertical cross-section. Although the overall trend of concentration is similar, the absolute errors vary noticeably across points, with the largest deviation observed at 4<sup>th</sup> point. This suggests that while both models capture the dispersion behavior qualitatively, the Gaussian model, using empirical dispersion parameters, may under- or overestimate concentrations

compared to the more physically-based Lagrangian formulation. The mean absolute error (MAE) of  $4.853 \times 10^{-5}$  indicates generally close agreement but highlights that model choice can significantly affect local concentration estimates, especially in regions with strong gradients or near the source.

## 5 Conclusion

This study provides a comparative evaluation of two widely used air dispersion models—the analytical Gaussian Plume Model (GPM) and the Lagrangian Model (LM)—for predicting ground-level SO<sub>2</sub> concentrations from industrial stack emissions. Both models were implemented using identical emission and meteorological conditions to assess their accuracy and computational performance. The GPM, based on a steady-state analytical formulation, provides rapid computations and smooth, symmetrical plume patterns, making it well-suited for regulatory screening and preliminary assessments. However, it often overestimates concentrations near the source, especially under variable wind conditions, due to its simplified treatment of turbulence and neglect of along-wind diffusion. In contrast, the LM solves time-dependent partial differential equations that account for evolving wind fields and spatially varying turbulence. This enables a more accurate representation of pollutant transport and dispersion, particularly under dynamic atmospheric conditions. Cross-sectional and vertical concentration profiles, as well as quantitative performance metrics such as RMSE, relative error, and Wasserstein Distance, highlight the LM's improved ability to replicate observed dispersion patterns. While the GPM offers advantages in simplicity and computational speed, the LM is more suitable for applications requiring higher resolution, temporal variability, and enhanced accuracy. Overall, these findings highlight the importance of selecting an appropriate dispersion model based on the specific goals of the air quality assessment, with a necessary trade-off between computational efficiency and predictive accuracy.

## References

- [1] G.I. Taylor. Diffusion by continuous movements. *Proceedings of the London Mathematical Society*, 20:196–212, 1921.
- [2] O.G. Sutton. The theoretical distribution of air-borne pollution from factory chimneys. *Quarterly Journal of the Royal Meteorological Society*, 73:426–436, 1947.
- [3] F. Pasquill. The estimation of the dispersion of windborne material. *Meteorological Magazine*, 90:33–49, 1961.
- [4] U.S. Environmental Protection Agency. Industrial source complex (isc) model. Technical report, U.S. EPA, 1976.
- [5] U.S. Environmental Protection Agency. Aermod: Description of model formulation. Technical report, U.S. EPA, 2004.
- [6] L. Zhang et al. Hybrid dispersion modeling approaches. *Atmospheric Environment*, 44(25):2945–2956, 2010.
- [7] N.S. Holmes. A review of the development and applications of gaussian plume models. *Environmental Science: Processes & Impacts*, 17:518–529, 2015.
- [8] Ádám Leelácssy, Ferenc Molnár, Ferenc Izsák, Ágnes Havasi, István Lagzi, and Róbert Mátyás. Dispersion modeling of air pollutants in the atmosphere: a review. *Central European Journal of Geosciences*, 6:257–278, 2014. doi:10.2478/s13533-012-0188-6.
- [9] Alex De Visscher. *Air Dispersion Modeling: Foundations and Applications*. Wiley, 2014.
- [10] Alice Crawford. The use of gaussian mixture models with atmospheric lagrangian particle dispersion models for density estimation and feature identification. *Atmosphere*, 11(12):1369, 2020.
- [11] D. Hryb, M. Cardozo, S. Ferro, and M. Goldschmit. Particle transport in turbulent flow using both lagrangian and eulerian formulations. *International Communications in Heat and Mass Transfer*, 36(5):451–457, 2009. doi:https://doi.org/10.1016/j.icheatmasstransfer.2009.01.017.
- [12] John J Walton. Scale-dependent diffusion. *Journal of Applied Meteorology (1962-1982)*, 12(3):547–549, 1973.
- [13] DJ Thomson. A stochastic model for the motion of particle pairs in isotropic high-reynolds-number turbulence, and its application to the problem of concentration variance. *Journal of fluid mechanics*, 210:113–153, 1990.
- [14] Andreas Stohl. Computation, accuracy and applications of trajectories. *Atmospheric Environment*, 32(6):947–966, 1998.
- [15] Andreas Stohl and David J Thomson. A density correction for lagrangian particle dispersion models. *Boundary-Layer Meteorology*, 90:155–167, 1999.
- [16] P Seibert and A Frank. Source-receptor matrix calculation with a lagrangian particle dispersion model in backward mode. *Atmospheric Chemistry and Physics*, 4(1):51–63, 2004.
- [17] Dmitrii Kochkov, Jamie A Smith, Ayya Alieva, Qing Wang, Michael P Brenner, and Stephan Hoyer. Machine learning-accelerated computational fluid dynamics. *Proceedings of the National Academy of Sciences*, 118(21):e2101784118, 2021.

- [18] Giovanni Bonafé, Francesco Montanari, and Fulvio Stel. A hybrid eulerian-lagrangian-statistical approach to evaluate air quality in a mixed residential-industrial environment. *International Journal of Environment and Pollution*, 64(1-3):246–264, 2018.
- [19] Jeevan Kafle, Krishna Prasad Adhikari, Eeshwar Prasad Poudel, and Ramesh Raj Pant. Mathematical modeling of pollutants dispersion in the atmosphere. *Journal of Nepal Mathematical Society*, 7(1):61–70, 2024.
- [20] Spiru Paraschiv, Gelu Coman, and Lizica Simona Paraschiv. Simulation of plume dispersion emitted from industrial sources based on gaussian model. In *AIP Conference Proceedings*, volume 2123, page 020059. AIP Publishing LLC, 2019.
- [21] Sayan Kar and Murali Damodaran. Models for assessing air pollution in cities. The Eighth Asia-Pacific Conference on Wind Engineering, 2013.
- [22] John C Lin, Dominik Brunner, and Christoph Gerbig. Studying atmospheric transport through lagrangian models. *Eos, Transactions American Geophysical Union*, 92(21):177–178, 2011.
- [23] Ignacio Pisso, Espen Sollum, Henrik Grythe, Nina I Kristiansen, Massimo Cassiani, Sabine Eckhardt, Delia Arnold, Don Morton, Rona L Thompson, Christine D Groot Zwaafink, et al. The lagrangian particle dispersion model flexpart version 10.4. *Geoscientific Model Development*, 12(12):4955–4997, 2019.
- [24] Wm J Veigle and James H Head. Derivation of the gaussian plume model. *Journal of the Air Pollution Control Association*, 28(11):1139–1140, 1978.
- [25] D. Bruce Turner. *Workbook of Atmospheric Dispersion Estimates: An Introduction to Dispersion Modeling*. CRC Press, 1994.
- [26] Steven R. Hanna, Gary A. Briggs, and Ray P. Hosker Jr. *Handbook on Atmospheric Diffusion*. Technical Information Center, U.S. Department of Energy, 1982.
- [27] John H. Seinfeld and Spyros N. Pandis. *Atmospheric Chemistry and Physics: From Air Pollution to Climate Change*. John Wiley & Sons, 2016.
- [28] Daniela Buske, Marco Túllio Vilhena, Tiziano Tirabassi, and Bardo Bodmann. Air pollution steady-state advection-diffusion equation: the general three-dimensional solution. *Journal of Environmental Protection*, 3(9):1124–1134, 2012.
- [29] S. Pal Arya. *Air Pollution Meteorology and Dispersion*. Oxford University Press, 1999.
- [30] D.J. Thomson. *Criteria for the selection of stochastic models of particle trajectories in turbulent flows*, volume 180. 1987.
- [31] Howard C. Rodean. *Stochastic Lagrangian Models of Turbulent Diffusion*. American Meteorological Society, 1996.
- [32] Gary A. Briggs Steven R. Hanna and Robert P. Hosker Jr. *Handbook on Atmospheric Diffusion*. U.S. Department of Energy, 1982.
- [33] Paolo Zannetti. *Air Pollution Modeling: Theories, Computational Methods and Available Software*. Van Nostrand Reinhold, 1990.
- [34] D.B. Turner. *Workbook of Atmospheric Dispersion Estimates: An Introduction to Dispersion Modeling*. CRC Press, 1994.
- [35] James D. Wilson and Brian L. Sawford. Review of lagrangian stochastic models for trajectories in the turbulent atmosphere. *Boundary-Layer Meteorology*, 78:191–210, 2001.